10362 *Biochemistry* **2009,** *48,* 10362–10371
DOI: 10.1021/bi901249d

BIOCHEMISTRY
including biophysical chemistry & molecular biology
Article

Role of Tryptophan−Tryptophan Interactions in Trpzip β-Hairpin Formation, Structure, and Stability[†]

Ling Wu, Dan McElheny, Rong Huang, and Timothy A. Keiderling*

Department of Chemistry, University of Illinois at Chicago, 845 West Taylor Street, Chicago, Illinois 60607-7061.

Received July 21, 2009; Revised Manuscript Received September 29, 2009

ABSTRACT: A series of β-hairpin peptides based on variations of the TrpZip2 sequence, SWTWENGKWTWK, of Cochran and co-workers were studied using electronic circular dichroism (CD) and infrared (IR) spectra by varying temperature and pH. Selected tryptophan residues were substituted with Val to test the impact of specific Trp interactions on hairpin stability. Native-state structures of two of the variants were determined using 2-D NMR and shown to have the same cross-strand edge-to-face Trp−Trp interaction as in Trpzip2. Thermally induced conformational changes of the hairpins formed with these various sequences were studied with CD and IR. Thermodynamic analyses of the temperature variation of both IR (as analyzed using the amide I′ frequency shift) and CD (intensity) spectra were fit to a two-state model that yielded different T_m values, consistent with a multistate process of folding/unfolding. At low pH these differences were minimized, suggesting a change in the energetics. Cross-strand interacting Trp residues with an edge-to-face orientation had the strongest impact on hairpin stability, as judged by CD and IR data. The diagonal interaction between Trp2 and Trp9, which have a more parallel orientation in Trpzip2, contribute to the spectral response but do not independently stabilize the structure. Comparative study of these various physical interactions emphasizes the complex folding pathways that are important even for these small peptides.

The simplest model of a β-sheet is the β-hairpin structure consisting of a single sequence folded back on itself to generate two antiparallel strands coupled by a turn or a loop. In proteins, β-hairpins can be found in isolation, in a sequence to form a sheet, or stabilized by interaction with other structural elements. The study of β-hairpin structure and stability is of wide interest in part because hairpins have been proposed to act as nucleation sites for protein folding, both by providing a framework for and by participating in formation of hydrophobic cores (*1*−*9*). Additionally, understanding β-sheet structure and formation is biomedically relevant because of the underlying β-structures characterizing protein aggregates, which have a role in many pathological diseases (*10*). In contrast, the β-hairpin provides a structurally more controllable system where only two strands interact, rather than forming an ensemble of structures as is characteristic of an aggregation process. Thus hairpins provide an appropriate system for theoretical modeling and detailed analysis of spectra−structure relations.

Folding of β-hairpins can be initiated either by formation of a turn, which utilizes specific residue sequences and thereby brings the strands together, or by interaction of opposing residues on the two strand segments, which stabilizes the resulting compact state and allows the turn to form, as has been the subject of many studies (*4*, *11*−*13*). The latter mechanism is often promoted by hydrophobic collapse of separated residues in the sequence leading to cross-strand hydrogen bond formation in the resulting dehydrated cluster with loop and turn formation following that in a sequence of steps. In contrast to this sequence of structure development from the middle to the outside, the turn-initiated mechanism is likely to be a zipping process of forming hydrogen bonds starting from residues adjacent to the turn, but alternate processes are possible (*2*, *14*). Some recent studies indicate that a mixture of these two mechanisms is likely to be operative (*15*, *16*).

Designs of sequences that form model β-hairpin peptides which are stable in water have taken two routes (or some combination of both) based on these mechanistic models, stimulating hairpin formation by turn stabilization or by hydrophobic coupling of cross-strand residues (*1*, *4*, *17*−*19*). Such hairpin sequences have often included nonproteinogenic residues to constrain the stereochemistry, thereby enhancing strand interactions. Many of these have yielded at least partial hairpin formation, but their thermal denaturation studies have often been characterized by broad unfolding transitions (*5*, *20*, *21*). Increasing the number of interstrand hydrophobic interactions has been shown to stabilize structures and result in hairpins that exhibit more sigmoidal denaturation profiles (*1*, *11*, *16*, *18*, *22*, *23*), but this hydrophobicity can also lower solubility and increase the risk of intermolecular aggregation.

Hydrophobic interactions have led to formation of some of the most stable β-hairpin models, particularly with the tryptophan zipper (Trpzip) models of Cochran and co-workers (*1*). These have been analyzed by study of thermodynamic stability using CD[1] and IR for tertiary and secondary structure transitions, respectively (*1*, *16*, *23*). Such spectral studies have been expanded

[†]This work was funded in part by grants from the National Science Foundation (CHE03-14016, CHE07-18543).

*To whom correspondence should be addressed: e-mail, tak@uic.edu; tel, 312-996-3156; fax, 312-996-0431.

[1]Abbreviations: CD, circular dichroism; IR, infrared; TOCSY, total correlation spectroscopy; NOESY, nuclear Overhauser enhancement spectroscopy.

 Published on Web 09/29/2009

to look at mechanistic aspects of the transition using relaxation kinetic data obtained from temperature jump (T-jump) experiments (*16*, *24*−*26*). In a series of related studies, Waters and coworkers have studied the impact of aromatic residues at various positions in the hairpin and have determined that Trp has an unusually high stabilizing impact in several positions (*27*, *28*). Previously, Fauve et al. (*29*) studied a series of small cyclic peptides with turns stabilized by a D-Pro-L-Pro template, one of which showed the same Trp−Trp edge-to-face ("T stack") geometry as in Trpzip. Subsequently, several other papers have appeared studying the effect of Trp−Trp interactions in peptide structures (*30*−*34*). This work suggested Trp−Trp was a means of creating more stable designs and led to our interest in further probing the pairwise Trp−Trp interaction and its impact on the hairpin stability. The impact of turn stability on hairpins has also been studied (*1*), and our parallel studies on the impact of variation of turn residues in Trpzip peptides will be presented separately.

Electronic circular dichroism (CD) spectroscopy can in principle be used to study β-sheet formation. However, in the 200−230 nm region, β-structures develop only a weak amide CD as compared to α-helices, and β-hairpins sometimes develop nonunique CD band shapes (*5*, *35*, *36*). Thus β-structure CD contributions can be easily obscured by contributions from aromatic groups, such as one might incorporate to promote a hydrophobic collapse. In the TrpZip hairpins, the pairwise Trp−Trp interactions result in a strong exciton CD signal (an intense derivative shape due to the π−π* dipole coupling) that indicates a distinctive cross-strand contact, effectively a tertiary structure. When the hairpin unfolds, this coupling is lost, and without a specific geometry the aromatic side chains generate little chirality. The observed CD then reverts back to that of a peptide amide chain in a "random coil" conformation, which is locally similar to poly-proline II, or an extended left-handed twist (*37*, *38*).

By contrast, vibrational spectra, especially that measured in the amide I′ region (C═O stretch vibration), have advantages for β-sheet determination (*39*−*41*). The amide I′ IR band for β-sheet proteins and peptides is distinct from other secondary structure types in both band shape and frequency position of the maximum intensity (*42*). This pattern can be found in the spectra of TrpZip molecules at low temperatures and, with temperature increase, reverts to a form (frequency shift and broadening) more characteristic of disordered structures (*16*, *23*−*26*). Optical spectra allow us to monitor the folding and unfolding of these hairpins and determine thermodynamic properties, assuming a model for the process, and enable evaluation of the relative stabilities for different sequences. Comparison of CD and IR results allows separate monitoring of tertiary and secondary structure formation, respectively.

We have previously reported studies of equilibrium and kinetic unfolding of the Trpzip2 hairpin, designed by Cochran et al. (*1*): Ser-Trp-Thr-Trp-Glu-Asn-Gly-Lys-Trp-Thr-Trp-Lys (SWTWENGKWTWK; TrpZip2), with all four Trps but minor modifications for isotopic labeling (*23*, *26*). Here we report studies of TrpZip2 related sequences where the three sets of Trp−Trp interactions are pairwise substituted by Val residues, first on the outer cross-strand pair (positions 2−11), then the inner pair (positions 4−9), and finally on the diagonal pair (positions 2−9). An independent study by Takekiyo et al. used alternate substitution patterns of Tyr for Trp on the TrpZip1 sequence, while pursuing a related goal (*43*).

Table 1: Comparative Sequences of Peptides Used for This Study[a]

peptide	sequence
Trpzip2	SWTWENGKWTWK-NH_2
W4W9	S**V**TWENGKWT**V**K
W2W11	SW**V**TVENGK**V**TW**V**K
W2W9	SWT**V**ENGKW**V**T**V**K

[a]Bold and underlines represent the mutated position.

The solution-phase structure of the parent peptide has been determined based on NMR analyses, which we have subsequently confirmed (*1*, *23*, *44*). TrpZip2 adopts a well-defined β-hairpin conformation with a type I′ β-turn at residues 6 and 7 and a sharply twisted hydrogen-bonded pair of strands (residues 1−5 and 8−12) stabilized by cross-strand tryptophan interaction (two pairs packing edge to face). Since the side chains on one strand insert between sequential residues on the other, there is less contact between adjacent tryptophan pairs in a strand (*1*, *44*). As will be shown here, variation of the Trp residues to Val, maintaining hydrophobic but not aromatic interaction, has impact on both the structure and the thermodynamics.

MATERIALS AND METHODS

Peptide Synthesis and Purification. The variations of the Trpzip2 sequence studied here are termed W4W9, W2W11, and W2W9, each of which has two tryptophans on the indicated positions (out of the four, Trp2, Trp4, Trp9, and Trp11, in the Trpzip2 sequence; see Table 1), the other two positions being substituted by Val. These mutants were originally obtained from GenScript Corp. Peptide TZ2 was synthesized in house using standard Fmoc-based solid-state synthesis methods. In this process, four equivalents of amino acid was activated with TBTU, HOBt (final concentration of 0.25M), and diisopropylethylamine (DIEA) at a final concentration of 0.5 M. A stepwise coupling of each amino acid was obtained using standard solid-phase Fmoc coupling chemistry. Once the synthesis was complete, the peptide was removed from solid-phase resin using a cleavage cocktail (by dissolving in 88:5:5:2 TFA/phenol/water/TIPS for 2 h). Crude peptides were isolated by precipitation into 10 volumes of cold ether, purified by reverse-phase HPLC (Vydac 218TP510 reversed-phase column), and characterized by MALDI-MS. The Trpzip2 mutants studied here are diagramed in Scheme 1, and their sequences are listed in Table 1.

NMR Spectra and Structure Analysis. We measured the NMR spectra of both W4W9 and W2W11 for ~4 mM (~5 mg/mL) concentrations in 20 mM phosphate buffer (90% H_2O and 10% D_2O) at pH 5.8. Spectra for structure determination were acquired at 281 K on a Bruker Avance 800 MHz spectrometer with gradient selection and excitation sculpting for water suppression (*45*). 2-D NOESY were acquired (mixing times = 80 and 300 ms) with 12 ppm sweep widths, 2048 × 1024 complex points in $t_2 \times t_1$ and 16 scans per increment. 2-D TOCSY were acquired under similar conditions with DIPSI2 mixing of 70 ms and a radio-frequency field of 8 kHz. All spectra were processed within NMRPipe (*46*) and viewed/assigned in NMRView (*47*).

The NOESY peaks were manually selected and assigned with CYANA 2.0 (*48*). The 100 lowest energy structures were selected from an ensemble of 500 and further refined by restrained MD using a previously described methodology within AMBER 8 (*49*). We used the ff99sb force field (*50*) plus the SHIFTS restraint (*51*) for the Trp rings with a force constant of 10 kcal/mol. The

Scheme 1: Sequences Showing Trpzip2, TZ2 (black), and the Mutant Peptides with Two Trp's Remaining, One on Each Strand: W4W9 (Blue), W2W11 (Pink), and W2W9 (Green)

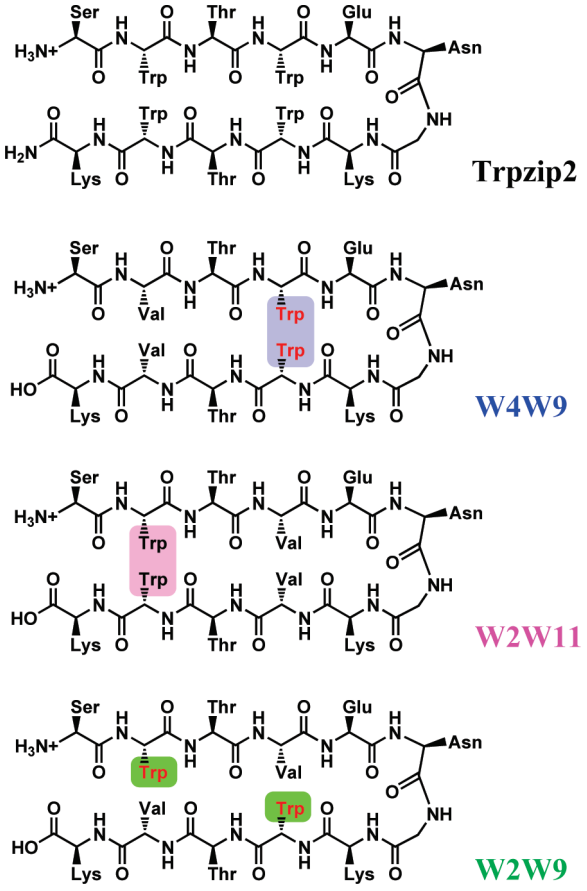

resulting 20 unique structures with the lowest AMBER and restraint violation energies were subjected to structure validation within PROCHECK_NMR (*52*).

CD Sample Preparation and Spectral Parameters. For CD experiments, peptide solutions were prepared at ~0.2 mg/mL (~0.13 mM) in 20 mM phosphate buffer (pH = 7 and pH ≈ 2). Far-UV CD spectra were acquired between 185 and 260 nm at 50 nm/min, with a 1 nm bandwidth and 2 s response time on a Jasco J-810 spectrometer using a 1 mm quartz cell (Starna, Inc.). Determination of sample concentration was based on absorbance at 280 nm (Trp ε_{280}: 5560 M^{-1} cm^{-1}). Final spectra were recorded as an average of eight scans and baseline subtracted. Variable-temperature experiments were done with a 1 °C/min ramp speed and a 5 min equilibration time, the temperature controlled by flow from a water bath (Neslab RTE7DP). Spectra over the range of 5−85 °C (in steps of 5 °C) were obtained for sample and buffer (for baseline subtraction) under identical experimental conditions. No smoothing was performed on the spectra. The CD amplitude variation with temperature was fit to a two-state model that used a linear folded (low temperature) and a flat unfolded (high temperature) baseline with $\Delta C_p = 0$ (*23*). [It should be noted that use of the $\Delta C_p = 0$ parameter is a result of the fact that inclusion of a variable ΔC_p in the fit resulted in very large errors for T_m and values of ΔC_p that were much smaller than the error. Examples are provided in the Supporting Information, Tables S2−S4. Thus ΔC_p is undetermined by our data.]

IR Sample Preparation and Spectral Parameters. Purified peptides were lyophilized twice against 0.1 M DCl/D_2O solution (both DCl and D_2O obtained from Sigma) to remove TFA counterions remaining from the peptide synthesis and then redissolved in D_2O, neutralized by NaOD, and lyophilized again. Equilibrium IR measurements have been carried out at different pH values to evaluate pH effects on the peptide structure and its un/refolding processes. Peptide solutions for IR studies were prepared in a range of concentrations, ~5−25 mg/mL (~3−17 mM), by dissolving lyophilized peptides in D_2O and adjusting pH with 20 mM deuterated phosphate buffer (to get pH ~ 7) and DCl (to get pH ~ 2).

IR spectra were acquired on a DigiLab FTS-60A spectrometer (Randolf, MA). Peptide solutions were sealed in a homemade demountable cell with CaF_2 windows separated by a 100 μm Teflon spacer. Sample and background spectra were collected at 4 cm^{-1} resolution with a zero-filling factor of 8. Temperature-variation experiments were conducted by placing the sample in a homemade cell holder stabilized at selected temperatures from 5 to 90 °C by flow from a bath (Neslab RTE 111). The sample was heated in 5 °C steps and equilibrated, and then 940 coadded scans were accumulated before the next temperature step.

RESULTS

Characterization of Tryptophan Mutant Peptide Structures. To determine the structure of the investigated peptides, NMR spectra including TOCSY and NOESY were measured (see Supporting Information, Figure S1). The observed NOEs are uniquely related to the β-hairpin structure. Cross-strand NOEs between atoms on the peptide backbone and lying near the Trp−Trp pair position are indicated by arrows in the molecular schemes below the NOESY plots. W2W11 (Trps near the termini) developed clearer and more extensive cross-strand NOEs than W4W9 (Trps near the turn), which implies that a strong Trp−Trp interaction at the 2 and 11 positions can draw the β-strands closer, locking the hairpin. These appear to be more effective, in terms of hairpin stabilization, than the pair at the 4 and 9 positions, which presumably lock in the turn and initiate hairpin formation.

Similar to what we have found for TZ2 (*23*), qualitative analysis of the chemical shifts (chemical shift index) for the H_α and amide resonances of W4W9 and W2W11 is also consistent with their having β-hairpin structures. Residues in the strand segments for W4W9 and W2W11 generally evidence a downfield shift of their H_α proton resonances from random coil values, whereas residues in the turn are shifted upfield more than 0.1 ppm, indicating formation of a β-hairpin (see Supporting Information, Figure S2) (*53*, *54*). However, the positive shifts in the W2W11 strand H_α values are more extensive and continue up to the turn, while those for W4W9 become negative near the turn and suggest a deformation. The stabilities and extent of the β-hairpins are suggested by strong downfield shifts for the V4, E5, and K8 residues in W2W11, while in both TZ2 and W4W9 those have weak downfield or even upfield shifts. From this, W2W11 appears to have more well-formed β-strands than do TZ2 and W4W9 and a somewhat different turn geometry, while TZ2 and W4W9 are suggested to have quite similar turn structures. This is borne out in our structure determination, below.

By contrast, W2W9 did not show any clear evidence of β-hairpin formation in terms of H_α chemical shift, indicating a globally random coil (disordered) conformation. The W2W9 chemical shifts at the N6 and K8 positions may indicate a residual population of turn residues.

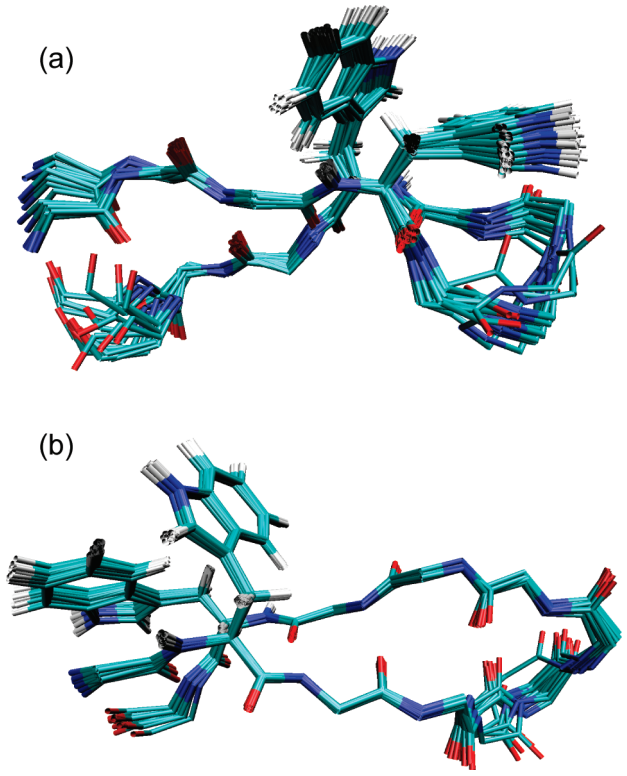

FIGURE 1: Peptide backbone overlap of 20 best NMR structures determined for (a) W4W9 and (b) W2W11. Structures are aligned for the residue 2−4 and 8−11 positions. Additionally shown are the Trp side chain interaction (pairwise, edge to face). Other side chains are removed from the figures for clarity. Note the variation in turn structure at Glu5-Asn6 in W2W11 (b).

Optimizations of the solution structures to fit our NMR data were undertaken to confirm these experimental observations. A simulated annealing protocol was used in conjunction with constraints based on the NMR chemical shift and NOE data to generate a number of low-energy structures for these β-hairpins. Relevant information used for and obtained from our structure determinations, indicating distance restraints from NOE and rms deviations from an ideal covalent geometry, is listed in the Supporting Information, Table S1. An overlap of the 20 lowest energy structures obtained from this analysis for W4W9 and W2W11 is shown in panels a and b of Figure 1, respectively. These structures show a high level of overlap in the center of the β-strand, and the variations at the termini (fraying) and turn (distortions) reflect the relative stabilities we have found spectroscopically (see following section). The ^{1}H chemical shifts of W4W9 and W2W11 in 20 mM phosphate buffer (H_2O with 10% D_2O) have been deposited in the BioMagResBank (http://www.bmrb.wisc.edu), BMRB accession numbers 16399 and 16407, respectively, and structural details are available from the authors.

The side-chain orientations of the Trp pairs in W4W9 and W2W11 shown in Figure 1 closely follow those determined for Trpzip2 NMR structures (*1*, *23*, *44*). They maintain the relative Trp−Trp geometries with high agreement in the overlap, and computations based on these geometries yield CD patterns that fit those seen experimentally (see below). Both pairs are determined to be oriented with one Trp indole ring packing edge-on to the face of the other Trp indole ring (~84° between indole planes) as seen for both pairs in Trpzip2. Other side chains show increasing disorder, but the Val (4 and 9 or 2 and 11) and Thr (3 and 10) are surprisingly regular (especially in W2W11; see Supporting Information Figure S3).

As compared to W2W11, the W4W9 structure (Figure 1a) has more twist, much more fraying at the termini, and more dispersion in the turn overlap, yet most of these 20 structures evidence type I′ turns, as seen in Trpzip2. By contrast, the 20 lowest energy structures for W2W11 (Figure 1b) overlay better and have more extended β-strands, but their β-turn residues evidence two distinct populations with variations centered on the Glu5 (ψ) and Asn6 (ϕ, ψ) angles. A survey of our 100 best structures for W2W11 shows a bimodal distribution in the Glu5 ψ and Asn6 ϕ values that encompasses these two structural types as shown in the Ramachandran plot in the Supporting Information, Figure S4. That these are reliable representations of the two types of turns is further supported by there being more NOEs for W2W11 than W4W9 or even for Trpzip2, the latter of which have one (the same) turn geometry (see Supporting Information, Figure S5). All of these structural characteristics are consistent with our experimental spectroscopic data, as detailed below.

Native-State Spectral Properties of Tryptophan Mutant Peptides. Trpzip2 has an unusual CD spectrum with intense exciton-coupled Trp $\pi-\pi^*$ bands at 213 and 228 nm, which indicate a tertiary-structure-like interaction between the aromatic chromophores but, due to spectral overlap with amide transitions, allow no insight into the peptide secondary structure (*23*). [Compared to this strong dipole coupling CD band, the amide contribution is much weaker in intensity.] In Trpzip2 two Trp pairs couple cross-strand at positions 4−9 and 2−11, and two diagonally related tryptophans, 2−9, also can couple. These assertions follow from our model TD-DFT calculations of the aromatic CD, based on the relative geometries of the Trp indole rings as determined from the Trpzip2 NMR structure, which are detailed separately in our previous work (*23*, *55*). W4W9 and W2W11, with just one pair of cross-strand coupled Trps, have the same experimental CD band shape as Trpzip2, evidencing strong negative−positive Trp $\pi-\pi^*$ exciton-coupled bands, but have about one-third the band intensity of Trpzip2 (see Figure 2). W2W9, with a potential diagonal cross-strand Trp−Trp interaction, does not exhibit exciton-coupled Trp bands in CD but rather shows a broad negative band at ~198 nm, consistent with amide CD arising from a mostly disordered secondary structure. [Computationally, CD of indoles in the TZ2 W2W9 geometry have the same sign and similar magnitude as for W2W11 and W4W9 but are shifted higher in frequency (*55*).]

IR spectra of the amide I′ mode (C═O stretch) primarily reflect the dominant secondary structure forms in a peptide. At neutral pH, W4W9 and W2W11 have similar amide I′ (D_2O solution) band shapes at 5 °C, a broadened, intense band whose maximum is at ~1632 cm^{-1} and a weak band at ~1675 cm^{-1} evident as a shoulder, which are consistent with formation of partial antiparallel β-sheet cross-strand interaction. As compared to Trpzip2, these are somewhat broader, and the lower energy component is shifted down by ~5 cm^{-1} (see Figure 3). By contrast, W2W9 has a qualitatively similar shape but is significantly broadened, and the lower component is shifted up in wavenumber as a result of a reduced amide I exciton splitting for any remaining β-strand structure (intense 1637 cm^{-1} and weak 1671 cm^{-1}). Thus the lack of exciton CD for W2W9 (Figure 2) is reflected in a band shape difference for the IR (corresponding to reduced vibrational exciton coupling), both indicating reduced β-hairpin formation. In practice, the observable IR absorbance intensity is limited by the peptide solubility in water, so the

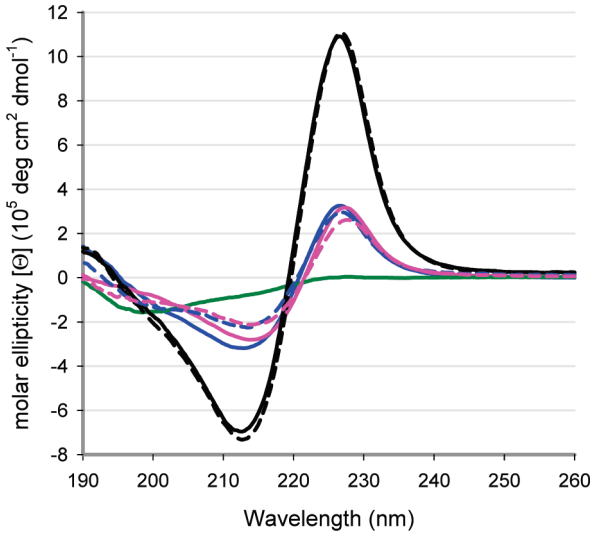

FIGURE 2: CD spectra of Trpzip2 and the mutant peptides W4W9, W2W11, and W2W9 measured at 5 °C at different pHs. Peptide concentration is ~0.2 mg/mL in 20 mM phosphate buffer (pH = 7). The path length of the cell is 1 mm. Vertical axis was corrected to molar ellipticity on a per molecule basis using solution concentrations determined by UV absorbance at 280 nm. Trpzip2 (black), W4W9 (blue), W2W11 (pink), and W2W9 (green), see Table 1. Corresponding dashed lines are for pH ≈ 2.

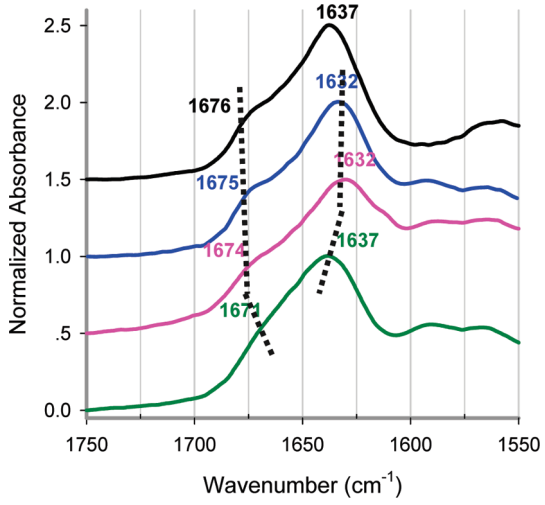

FIGURE 3: IR spectra of TZ2, W4W9, W2W11, and W2W9 measured in 20 mM deuterated phosphate buffer under neutral pH (pH = 7) at 5 °C. Sample concentrations were varied to account for their different solubilities: TZ2, 20 mg/mL; W4W9, 20 mg/mL; W2W11, 5 mg/mL; W2W9, 10 mg/mL. The path length of all samples was 100 μm. Spectra were normalized to a maximum absorbance of 1 from their measured maxima of 0.22 for TZ2 (black), 0.13 for W4W9 (blue), 0.07 for W2W11 (pink), and 0.11 for W2W9 (green).

spectra were normalized to a constant absorbance maximum just for comparison (original absorbance values are given in the caption). W4W9, with two Trps near the turn, is relatively soluble in water, while W2W11 and W2W9 are less so. Consequently, IR spectra of W4W9 were measured at ~20 mg/mL, while W2W9 were measured at ~10 mg/mL, the limit of its solubility in D_2O, and W2W11 at ~5 mg/mL.

There is a big difference in concentration between the CD and IR studies. In our previous study (*23*), CD spectra for Trpzip2 variants over a range from 0.1 to 7 mg/mL were shown to have no change in the CD band shapes. In addition, we carried out a comparative NMR TOCSY study for W2W11 (the least soluble sample) at 0.6 and 6.0 mg/mL, that resulted in complete overlap of the resolved features (Supporting Information, Figure S6).

Thermal Unfolding of Tryptophan Mutant Peptides. The thermal stability of the Trp−Trp interaction for W4W9 in phosphate buffer (pH ≈ 7) was monitored by variable-temperature CD (Figure 4a). For both W2W11 and W4W9 with increasing temperature, the strong negative−positive tryptophan exciton-coupled bands at 213 and 228 nm almost vanish at higher temperatures while a weak negative band at 198 nm, characteristic of disordered peptides (amide $\pi-\pi^*$), appears as temperature increases from 5 to 85 °C. This suggests a loss of Trp−Trp interaction and increase in the fraction of disordered peptide conformation at the same time. The intensity loss of both the 213 nm negative and 228 nm positive peaks with increasing T was measured to yield thermal transition curves, which were then fit to a two-state model that used a linear folded and flat unfolded baseline with $\Delta C_p = 0$ (*23*). These constraints were chosen to yield the best fits, within acceptable errors. The errors for ΔC_p make it undetermined (essentially zero, which is why it was fixed for the best fits) with our data (see Supporting Information, Tables S2−4). Intensity loss at 228 nm with temperature for TZ2 and the cross-strand Trp pair mutants, W4W9 and W2W11, is plotted in Figure 4b.

As monitored by CD, W4W9 and W2W11 have similar stabilities, evidenced by T_m ~342 K for W4W9 and ~347 K for W2W11, both of which are lower than the T_m for the parent peptide, Trpzip2 (~352 K, using the same analysis method, Table 2). The broad thermal transitions for the mutants show little curvature and suggest that these peptides are not fully folded at low temperature and may not undergo a simple two-state unfolding process. However, the quality of our NMR data suggests the unfolded population is low for W2W11 and W4W9. The high-temperature band shape indicates that these peptides lose most of their Trp−Trp interaction on heating and is consistent with our detecting amide CD characteristic of a primarily disordered secondary structure for these peptides at 85 °C. Because the W2W9 CD at room temperature already indicates significant disorder, its thermal variation was not pursued.

The thermal stability of the secondary structure of W4W9, W2W11, and W2W9 in phosphate buffer was monitored by variable-temperature IR. The IR absorption maximum of W4W9 shifted from 1632 to 1645 cm^{-1} as temperature increased from 5 to 90 °C (see Figure 5a), corresponding to a secondary structural change from hairpin to mostly disordered that is correlated with the CD-detected tertiary structure change (Figure 4a). The intensity variation of W4W9 and W2W11 at ~1632 cm^{-1} (W2W9 at 1637 cm^{-1}), which corresponds to the amide I′ maximum at 5 °C and is characteristic of the β-strand contribution to the amide I′ hairpin IR, was fit for thermal analyses. At high temperature all yield a similar broad, symmetric amide I′ band with a maximum at ~1649 cm^{-1}, which is consistent with their all reaching a similar disordered state at 90 °C. The absorbance intensity measured for these peptides varied widely, reflecting the concentrations we could employ due to their solubility differences. To obtain an improved comparison, we plotted the IR intensity transition curve for TZ2 and the mutant peptides in Figure 5b by normalizing their maximum intensity to 1. [Since W2W9 is partially unfolded at low temperature, its change at 1637 cm^{-1} senses both β and disordered structures, and sensible comparison was not possible; thus it is not in Figure 5b.].

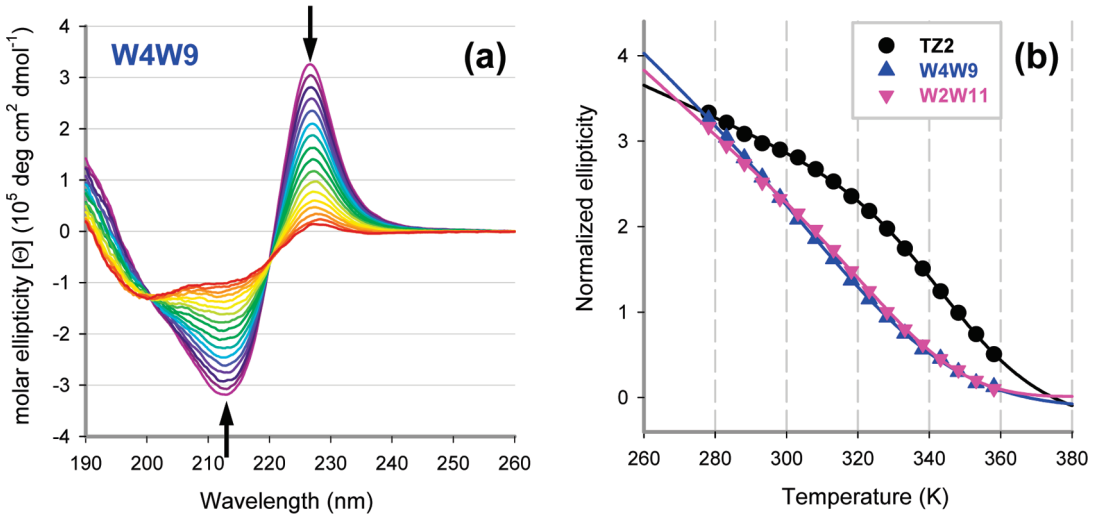

FIGURE 4: (a) Temperature-dependent CD spectra of tryptophan mutant peptides W4W9 measured from 5 to 85 °C, as described in Figure 2. Color changes indicate increasing temperature, from violet (cold) to red (hot). (b) Ellipticity changes for the positive exciton peak (~227 nm) of TZ2, W4W9, and W2W11. Maximum intensity of TZ2, W4W9, and W2W11 mutants was normalized to the same scale for comparison. These curves were fit to a two-state model assuming linear folded and flat unfolded baselines with $\Delta C_p = 0$ to determine the corresponding transition temperatures (*23*). TZ2 (black solid dot), W4W9 (blue solid up triangle), W2W11 (pink solid down triangle).

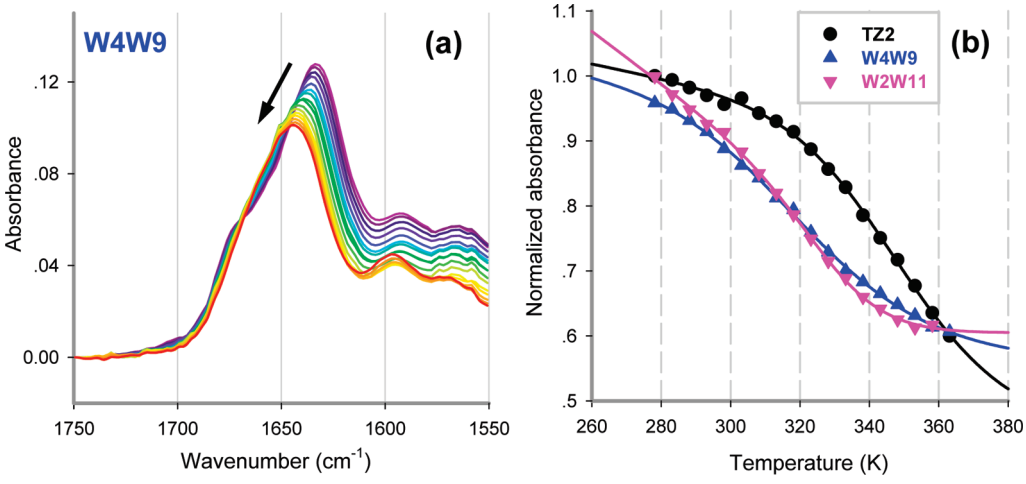

FIGURE 5: (a) Original temperature-dependent IR spectra for W4W9 measured as in Figure 3. (b) Two-state fit of the IR intensity change for TZ2 (black solid dot), W4W9 (blue solid up triangle), and W2W11 (pink solid down triangle) at 1637, 1632, and 1632 cm^{-1}, respectively, which correlates to the maxima of the β-strand contribution.

Table 2: Thermodynamic Parameters for the Two-State Model Fit of CD and IR Data at pH = 7[a]

	T_m (K)		ΔH (kcal·mol^{-1})		ΔS (cal·mol^{-1}·K^{-1})	
peptides	FTIR[b]	CD	FTIR	CD	FTIR	CD
Trpzip2	352 ± 3	352 ± 2[c]	15 ± 2	17 ± 2	43	48
W4W9	326 ± 7	342 ± 7	11 ± 1	10 ± 1	33	30
W2W11	332 ± 2	347 ± 4	18 ± 2	16 ± 2	54	46

[a]Linear-flat baseline two-state fitting model and $\Delta C_p = 0$ used for fit. [b]Absorbance at TZ2 1637 cm^{-1}, W4W9 1632 cm^{-1}, W2W11 1632 cm^{-1}, and W2W9 1637 cm^{-1} (Figure 5). [c]Unpublished data from UIC (consistent with Cochran's original data).

From the variable-temperature IR, we obtained $T_m \sim 326$ K for W4W9 and $T_m \sim 332$ K for W2W11, as summarized with the CD results in Table 2. [Attempts to fit the W2W9 IR yielded a considerably higher value, which is unlikely to be meaningful.]. As for CD, the T_m values for W2W11 and W4W9 are similar to each other and significantly lower than for Trpzip2; however, the absolute T_m values obtained for the mutant IR intensity changes are very different from the T_m values found with CD, providing further evidence that these two peptides do not follow a two-state thermal unfolding process. The baseline for the amide I band at pH ~ 7 is distorted on the low frequency side by overlap with the COO^- band. SVD (singular value decomposition) analysis of the data was used to separate the baseline component and fit the result. As shown in the Supporting Information, Table S5, the SVD has qualitatively the same result; the T_m's are closer to Trpzip2 values and to the CD values but still maintain a clear difference between Trpzip2 and the mutants. That the tertiary structure transition temperatures (CD) are higher than the secondary structure transition temperatures (IR) suggests that the pairwise Trp−Trp interaction between the strands may have more stability than the β-sheet backbone structure (cross-strand H-bonded component) which can partially unfold as temperature increases while still maintaining some Trp−Trp interaction.

pH Effect on Structure and Stability. In a previous study, we found that Trpzip2 at low pH has higher solubility and gives more reversible thermal transitions (*26*), so we investigated the effect of pH on hairpin stability. CD spectra of TZ2, W4W9, and W2W11 at 5 °C at both pH 7 and pH 2 (Figure 2) have the same Trp−Trp exciton band shape and comparable peak intensities, indicating that they have very similar geometries for the Trp pairs. The main difference is that the negative Trp exciton band at 218 nm is somewhat weaker at low pH than at neutral pH for W4W9 and W2W11, which have only one pair of Trps.

In the FTIR spectra, various components of the amide I arise from cross-strand β-coupled amides (~1630 and ~1680 cm^{-1}), β-turns (~1660−1675 cm^{-1}), and disordered amides (~1660 cm^{-1}), but these contributions cannot be fully resolved or uniquely assigned. Consequently, the amide I bands at different pH were fit to a sum of three components (see Supporting Information, Figure S7) with a high level of agreement yielding a consistent pattern of variation. The relative peak areas for the major (β and coil) components are compared in Figure 6, showing that all of the peptides have increased disorder at lower pH, which indicates a partial unfolding and destabilization of the secondary structure, whereas the similar CD spectral response at different pHs suggests the Trp−Trp interaction changes much less.

IR analysis shows W2W11 to have more β content and less coil content than W4W9 at neutral pH, consistent with less disorder for W2W11, as suggested by the NMR structural results (Figure 1). It also loses more β content and gains more coil content than W4W9 upon pH change. This indicates that pH has a larger effect on β-strand backbone structure when the Trp−Trp interaction is at the end of the strand (hence close to the uncapped termini where the C-terminal charge state changes) than when it is close to the turn, or conversely that the change is larger when there is more structure. The relative changes with pH and temperature also can be used to suggest interpretations for the role of aromatic coupling in stabilizing the hairpins (see next section). Consistent with the relative CD result (Figure 2), pH has less impact on the Trpzip2 peptide IR than for W2W11 or W4W9.

To further characterize the pH effect, we analyzed the temperature dependence of the exciton CD band and the FTIR amide I′ peak of these peptides at pH 2. The change in intensity for the positive CD band at ~228 nm for TZ2, W4W9, and W2W11 at different pH (Figure 7) monitors the tertiary structure unfolding. The CD thermal unfolding curves of all three peptides were shifted to lower temperature (open symbols) at lower pH, but the impact is much larger for W4W9 and W2W11 than for

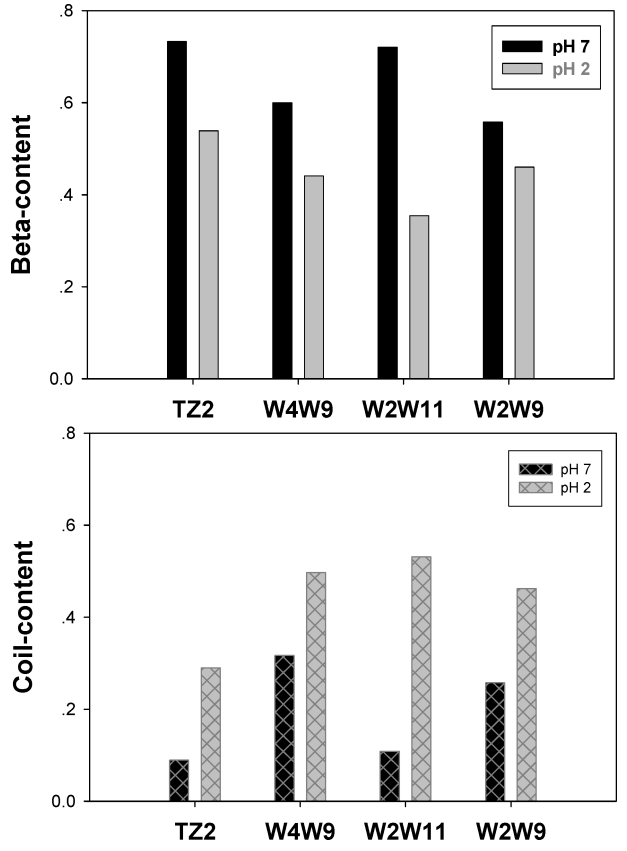

FIGURE 6: Comparison of β-content and random coil content at different pH values derived from the areas of the IR spectral deconvolutions in the Supporting Information, Figure S7. Bars for β-content represent the deconvolution peak at ~1630 cm^{-1}; coil content bars represent the deconvolution peak at ~1660 cm^{-1}. Neutal pH (black bar); acidic pH (gray bar).

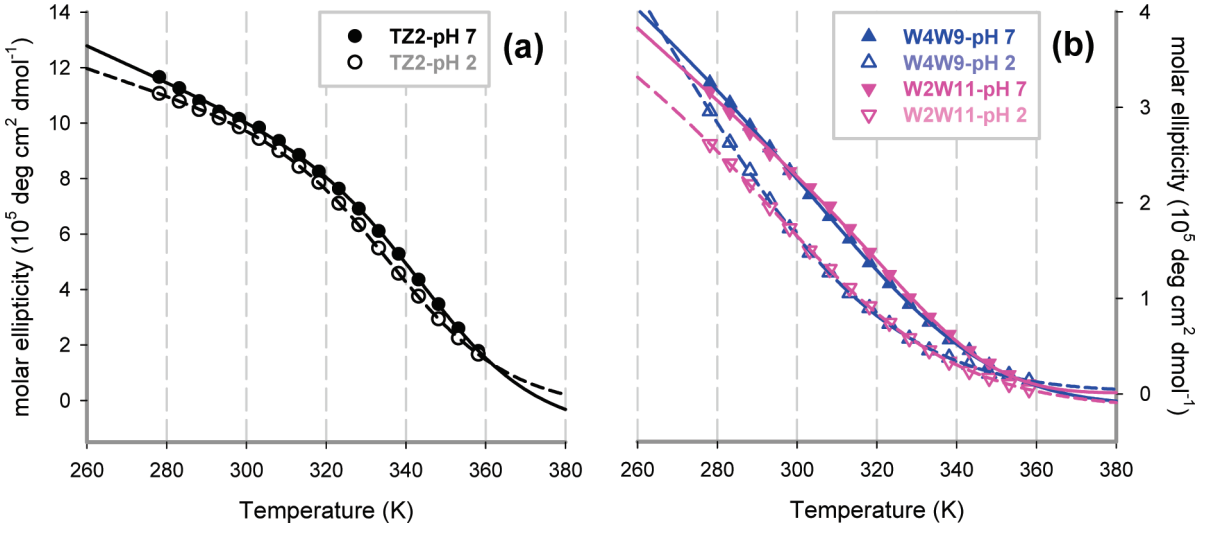

FIGURE 7: Comparison of CD transition curves of TZ2 and W4W9 and W2W11 mutants at different pH. (a) TZ2 (neutral pH, black solid dots; acidic pH, black open dots) and (b) W4W9 (neutral pH, blue solid up triangle; acidic pH, blue open up triangle) and W2W11 (neutral pH, pink solid down triangle; acidic pH, pink open down triangle). These curves were fit to a two-state model assuming a linear folded and flat unfolded baseline with $\Delta C_p = 0$ to get corresponding transition temperatures.

Table 3: Low pH Thermodynamic Parameters for the Two-State Model Fit of IR and CD Data[a]

	T_m (K)		ΔH (kcal·mol^{-1})		ΔS (cal·mol^{-1}·K^{-1})	
peptides, pH = 2	FTIR	CD	FTIR	CD	FTIR	CD
Trpzip2	340 ± 1	343 ± 0.3	14 ± 1	16 ± 0.3	41	46
W4W9	311 ± 4[b]	312 ± 11	−[b]	6 ± 0.9	−[b]	21
W2W11	317 ± 4	320 ± 7	14 ± 1	9 ± 0.3	45	27
W2W9	332 ± 4	N/A[c]	16 ± 3	−	50	−

[a]Linear-flat baseline two-state fitting model and $\Delta C_p = 0$ used for fits. [b]Transition curve does not show clear sigmoidal shape; fit with linear−linear baseline $\Delta C_p = 0$, but ΔH and ΔS for FTIR had very large error, not included. [c]No apparent exciton CD band for W2W9.

TZ2. TZ2 had T_m = 343 K at pH 2 or ~10 K lower than at pH 7, while W4W9 and W2W11 had T_m = 312 and 320 K, respectively, or ~30 K lower than at pH 7 (Table 3). Again, as at pH 7, W2W11 is more stable than W4W9, but at pH 2 both are much less stable than TZ2 as sensed by Trp−Trp interaction monitored with CD.

When the thermal transition is monitored by IR intensity variation at ~1638 cm^{-1} at low pH, we saw a somewhat different response. The W4W9 transition curve is nonsigmoidal, making the determined thermal parameters unreliable (also with SVD analysis). With the Trps closer to the turn, their interaction, and hence CD, can be maintained while the strands can fray sequentially as temperature is increased. These contributions distort the low temperature β-cross-strand H-bonding pattern that yields the band shape seen and the NMR structure determined. With IR analysis, all peptides show a lower T_m at lower pH than at neutral pH, by ~9−15 K (Table 3), which is consistent with but much smaller than the pH-induced T_m lowering found for the CD analyses. Consequently, at low pH, T_m for thermal transitions detected with IR and CD are about the same. However, the errors especially for W4W9 are quite large. This difference indicates pH has different impact on the mutant secondary and tertiary structure thermal stability than on TZ2.

DISCUSSION

Peptide Structure. We have shown that the mutant peptides W2W11 and W4W9 have qualitatively the same β-hairpin fold as does Trpzip2. Most importantly, they have virtually identical cross-strand Trp−Trp interaction geometries, which leads to the observed CD spectral response that is used to monitor the tertiary-like structure in this small, well-structured foldamer and results in a stable fold, unlike the diagonal interaction in W2W9 (potential), which does not form. The minor differences in stability between W2W11 and W4W9 are reflected in the higher quality of overlap between the low energy NMR structures and are consistently reflected in the thermal stabilities found in our IR and CD analyses. These structures show that the Trp−Trp interaction in W4W9 yields the same turn geometry as for Trpzip2, but both are somewhat distorted from a type I′ turn. Without having the close-lying Trp−Trp pair, the W2W11 turn develops two quite different turn structures, indicating that release of the constraint frees the turn to alternate between forms.

Impact of Trp−Trp Coupling on Stability. Cross-strand coupling of hydrophobic residues is an important factor in stabilizing β-hairpin models (*1*, *11*), and Waters et al. have shown that Trp interactions have a much bigger impact than do those of other residues (*18*, *27*, *28*, *56*, *57*). Andersen and co-workers have extensively reviewed such interactions and investigated a number of sequences with Trp substitutions in a careful extensive study (*31*). Using CD data, they also found poorly sigmoidal thermal transition curves which they referenced to assigned fully folded states in organic mixed solvents, which brings in a different dimension to the problem. Guvench and Brooks studied the edge-to-face interaction with MD simulations in Trpzip2 and showed it to be dependent on multipole interaction (*32*). Our results are consistent with the importance of Trp−Trp interactions but additionally show that the interactions are additive and have a geometrical aspect.

In the results presented above, the cross-strand couplings of pairs of Trps at the 4−9 and 2−11 positions appear to be very similar, but the diagonal coupling for Trps at positions 2−9 is different and much less effective in stabilizing the hairpin structure. This is evident in two ways. The CD spectra of W4W9 and of W2W11 are virtually identical, as would be expected from the near-identical relative geometries of the Trp−Trp pairs we have shown to be characteristic of each, but their CDs are much weaker (less than a third) than that of Trpzip2 (or Trpzip2C (*23*)). This could indicate added interaction between the inner residues (2−9) of the two pairs or added stability of the hairpin in TZ2 with four Trps interacting. The NMR structures for W4W9 and W2W11 indicate that both hairpins are well-formed in the β-strand segments resulting in the same relative Trp−Trp geometries, albeit with W4W9 showing more variation and having frayed termini. Since both have the same experimental CD spectra, and are computed to have very similar CD (*55*), the added stability (evidenced in higher T_m) does not seem to be the source of the higher CD intensity (a factor of 3) for Trpzip 2. The difference in CD thus appears to be an added interaction present with four Trps, primarily the W2W9 coupling.

Since the experimental W2W9 CD is a reasonable approximation to that of the unfolded hairpin, one might hypothesize that 2−9 coupling is not significant and that stability is the main factor in the resultant signal. Our TD-DFT calculational results, presented separately, show that four indole rings in the Trpzip2 geometry should have a CD intensity greater than twice that of two Trps in either the W2W11 or W4W9 geometries (*23*, *55*). In addition, the W2W9 interaction, which has a different geometry, would generate a significant CD spectrum of the same sign pattern. Thus theory does not support a weak interaction between these residues but rather a different, geometrically derived one. However, if the W2W9 did not form a stable hairpin structure at low temperature, which is consistent with our data, then there can be no significant coupling, and the contribution of the 2−9 positions cannot be evaluated from W2W9 CD spectra. This lack of structure in W2W9 is supported by its CD reflecting a random coil, its broadened and shifted amide I IR, and its C_α-H chemical shifts being closest to random coil values. Thus the structural variation between the mutants is clear in terms of Trp coupling.

With IR we can study the stability of the peptide backbone. Again, W4W9 and W2W11 have very similar band shapes consistent with cross-strand β-type H-bonding as found in our NMR structures. Thus by combining the IR and CD observations, one can determine that the lack of exciton CD in W2W9 is due to reduced Trp interaction caused by unfolding and is not an intrinsic geometrical phenomenon. Since the Trpzip2 CD

magnitudes are about three times those of W4W9 or W2W11, the W2W9 contribution must be a significant addition, implying that the four Trps in the TrpZip2 structure gain added exciton coupling from forming stable interactions between all the pairs. The Trpzip1 structure follows this same pattern, as we have shown separately (*43*), but is overall less stable.

Thermal Variations. Beyond spectral character, the CD and IR thermal variations bring out other characteristics. The W4W9 and W2W11 CD intensity changes with increasing temperature show broadened sigmoidal transitions that can be fit to a two-state model yielding similar transition temperatures of about T_m = 342 and 347 K, but with IR these drop to T_m = 326 and 332 K, respectively, all of which are well below the T_m = 352 K of the parent sequence, TrpZip2. The ΔH values for W2W11 and W4W9 differ in a way that parallels the T_m's for these peptides. For both IR and CD analyses the ΔH values for W2W11 are roughly the same as for Trpzip2, implying that the major change is loss of the well-formed cross-strand H-bonds. The W4W9 values are lower (Table 2), consistent with its reduced stability as compared to W2W11, as implied by the fraying and fewer NOE constraints found for its NMR structure.

The CD band profiles have clear isodichroic points as temperature varies, supporting use of the two-state model, which makes sense for Trp coupling, but the IR transitions have less well defined isosbestic points. Trpzip2 has the same T_m for IR and CD, which implies a cooperative unfolding between its Trp side-chain tertiary structure (CD) and β-hairpin backbone secondary structure (IR). When the Trp−Trp interaction is lost in Trpzip2, the secondary structure is so destabilized as to unfold. By contrast, W4W9 and W2W11 have significantly lower T_m values for thermal transitions monitored with IR than with CD, which indicates they can lose β-backbone structure (fray or distort strand alignment) more easily than break Trp−Trp coupling with temperature. In the mutant cases the mechanism is one of gradual β-backbone unfolding (breaking interstrand H-bonds) followed at some point by loss of the Trp−Trp coupling. It can be concluded that mutations of Trp to Val or aromatic to hydrophobic interaction made on TZ2 not only affect β-hairpin stability but also cause a different unfolding pathway (more fraying) to become accessible for W4W9 and W2W11 as compared to TZ2.

pH Effect on Peptide Structure and Unfolding Mechanism. With different pH values, TZ2, W4W9, and W2W11 have very similar CD shape and intensity in their native state (5 °C, Figure 2), which implies that low pH does not strongly impact the native-state Trp−Trp tertiary interaction. However, their secondary structure, as monitored with IR, does change, resulting in an increase in the degree of disordered structure at reduced pH (Figure 6). It should be noted that relative change has some reliability for these IR deconvolutions but the absolute value of the disordered fraction would also include contributions from residues in the turn due to our inability to resolve them. All four peptides lose β-structure and gain coil content at lower pH. The difference at lower pH may be due to change in charges on various residues that could destabilize a compact structure, but since the Trp side chains would not become additionally protonated at pH 2, they would have less change. While the Trpzip2 was C-terminally blocked, this probably has little impact, since W2W11 with charged termini is highly ordered as found earlier for Trpzip2 with C-terminal blocking, but W4W9 is less and is also unblocked.

The overall T_m's for the secondary structure (IR measurements) and tertiary structure (CD measurements) of TZ2 are the same at pH 7 and are ~10 K lower at pH 2. This means by lowering pH TZ2 becomes less stable and unfolds at a lower temperature. Still, TZ2 appears to lose secondary and tertiary structure in the same process at both pH values, which is why it also appears to adopt a two-state unfolding mechanism. The secondary structure is held together in TZ2 by the hydrophobic side-chain interaction, and when this is lost, the entire peptide can unfold. By contrast, the single Trp pair mutants, W4W9 and W2W11, have a higher T_m for CD and a lower T_m for IR at pH 7, while their T_m's for CD and IR are approximately the same at pH 2. This indicates that at neutral pH the secondary structure of W4W9 and W2W11 could unfold gradually as temperature increases. When the loss of oriented Trp interaction occurs, the multistep process goes to completion. However, at pH 2, both secondary and tertiary structures are lost in the same temperature range.

Put in another way, lowering pH changes the favored unfolding pathway for W4W9 and W2W11 to a more synchronous one. All of our observations point to a multistate unfolding process for Trpzip peptides, where the balance between the ordering of steps and population of different intermediates along the path is subject to environment. Shifting the number of contacts and the position of the interaction in the sequence both destabilizes the hairpin and allows alternate folding mechanistic steps to be energetically favorable.

ACKNOWLEDGMENT

We thank Anjan Roy and Petr Bour for sharing the results of their TD-DFT CD calculations before publication.

SUPPORTING INFORMATION AVAILABLE

Details of the NMR structure determinations, expanded structural fits, and comparative analyses of the CD and IR thermal data with different models. This material is available free of charge via the Internet at http://pubs.acs.org.

REFERENCES

1. Cochran, A. G., Skelton, N. J., and Starovasnik, M. A. (2001) Tryptophan zippers: stable, monomeric beta-hairpins. *Proc. Natl. Acad. Sci. U.S.A. 98*, 5578–5583.
2. Dinner, A. R., Lazaridis, T., and Karplus, M. (1999) Understanding β-hairpin formation. *Proc. Natl. Acad. Sci. U.S.A. 96*, 9068–9073.
3. Eaton, W. A., Munoz, V., Thompson, P. A., Henry, E. R., and Hofrichter, J. (1998) Kinetics and dynamics of loops, alpha-helices, beta-hairpins, and fast-folding proteins]. *Acc. Chem. Res. 31*, 745–753.
4. Gellman, S. H. (1998) Minimal model systems for β-sheet secondary structure in proteins. *Curr. Opin. Struct. Biol. 2*, 717–725.
5. Hilario, J., Kubelka, J., and Keiderling, T. A. (2003) Optical spectroscopic investigations of model beta-sheet hairpins in aqueous solution. *J. Am. Chem. Soc. 125*, 7562–7574.
6. Ma, B., and Nussinov, R. (2000) Molecular dynamics simulations of a β-hairpin fragment of protein G: balance between side-chain and backbone forces. *J. Mol. Biol. 296*, 1091–1104.
7. Maynard, A. J., Sharman, G. J., and Searle, M. S. (1998) Origin of β-hairpin stability in solution: structural and thermodynamic analysis of the folding of a model peptide supports hydrophobic stabilization in water. *J. Am. Chem. Soc. 120*, 1996–2007.
8. Munoz, V., Thompson, P. A., and Hofrichter, J. (1997) Folding dynamics and mechanism of beta-hairpin formation. *Nature 390*, 196–199.
9. Stanger, H. E., Syud, F. A., Espinosa, J. F., Giriat, I., Muir, T., and Gellman, S. H. (2001) Length-dependent stability and strand length limits in antiparallel β-sheet secondary structure. *Proc. Natl. Acad. Sci. U.S.A. 98*, 12015–12020.

10. Harper, J. D., and Lansbury, P. T. (1997) Models of amyloid seeding in Alzheimers desease and scrapie: mechanistic truths and physiological consequences of the time-dependent solubility of amyloid proteins. *Annu. Rev. Biochem. 66*, 385–407.
11. Hughes, R. M., and Waters, M. L. (2006) Model Systems for β-hairpins and β-sheets. *Curr. Opin. Struct. Biol. 16*, 514–524.
12. Blandl, T., Cochran, A. G., and Skelton, N. J. (2003) Turn stability in β-hairpin peptides: investigation of peptides containing 3:5 type I G1 bulge turns. *Protein Sci. 12*, 237–247.
13. Russell, S. J., and Cochran, A. G. (2000) Designing stable β-hairpin: energetic contributions from cross-strand residues. *J. Am. Chem. Soc. 122*, 12600–12601.
14. Munoz, V., Henry, E. R., Hofrichter, J., and Eaton, W. A. (1998) A statistical mechanical model for β-hairpin kinetics. *Proc. Natl. Acad. Sci. U.S.A. 95*, 5872–5879.
15. Deechongkit, S., Jager, M., Nguyen, H., Powers, E. T., Gruebele, M., and Kelly, J. W. (2006) β-Sheet folding mechanisms from pertubation energetics. *Curr. Opin. Struct. Biol. 16*, 94–101.
16. Yang, W., Pitera, J., Swope, W., and Gruebele, M. (2004) Multiple ensembles during trpzip unfolding probed by replica-exchange MD and experiment. *J. Mol. Biol. 336*, 241–251.
17. Ragothama, S. R., Awasthi, S. K., and Balaram, P. (1998) β-Hairpin nucleation by Pro-Gly β-turns. Comparison of D-Pro-Gly and L-Pro-Gly sequences in an apolar octapeptide. *J. Chem. Soc., Perkin Trans. 2*, 137–143.
18. Tatko, C., and Waters, M. (2002) Selective aromatic interactions in β-hairpin peptides. *J. Am. Chem. Soc. 124*, 9372–9373.
19. Russell, S. J., Blandl, T., Skelton, N. J., and Cochran, A. G. (2003) Stability of cyclic beta-hairpins: asymmetric contributions from side chains of a hydrogen-bonded cross-strand residue pair. *J. Am. Chem. Soc. 125*, 388–395.
20. Setnicka, V., Huang, R., Thomas, C. L., Etienne, M. A., Kubelka, J., Hammer, R. P., and Keiderling, T. A. (2005) IR study of cross-strand coupling in a β-hairpin peptide using isotopic labels. *J. Am. Chem. Soc. 127*, 4992–4993.
21. Huang, R., Setnicka, V., Etienne, M. A., Kim, J., Kubelka, J., Hammer, R. P., and Keiderling, T. A. (2007) Cross-strand coupling of a β-hairpin peptide stabilized with an Aib-Gly turn studied using isotope-edited IR spectroscopy. *J. Am. Chem. Soc. 129*, 13592–13603.
22. Du, D., Tucker, M. J., and Gai, F. (2006) Understanding the mechanism of β-hairpin folding via Φ-value analysis. *Biochemistry 45*, 2668–2678.
23. Huang, R., Wu, L., McElheny, D., Bour, P., Roy, A., and Keiderling, T. A. (2009) Cross-strand coupling and site-specific unfolding thermodynamics of a Trpzip β-hairpin peptide using ^{13}C isotopic labeling and IR spectroscopy. *J. Phys. Chem. B 113*, 5661–5674.
24. Du, D. G., Zhu, Y. J., Huang, C. Y., and Gai, F. (2004) Understanding the key factors that control the rate of β-hairpin folding. *Proc. Natl. Acad. Sci. U.S.A. 101*, 15915–15920.
25. Snow, C. D., Qiu, L., Du, D., Gai, F., Hagen, S. J., and Pande, V. S. (2004) Tryptophan zipper folding kinetics via molecular dynamics and temperature-jump spectroscopy. *Proc. Natl. Acad. Sci. U.S.A. 101*, 4077–4082.
26. Hauser, K., Krejtschi, C., Huang, R., Wu, L., and Keiderling, T. A. (2008) Site-specific relaxation kinetics of a tryptophan zipper hairpin peptide using temperature-jump IR spectroscopy and isotopic labeling. *J. Am. Chem. Soc. 130*, 2984–2992.
27. Waters, M. L. (2002) Aromatic interactions in model systems. *Curr. Opin. Struct. Biol. 6*, 736–741.
28. Waters, M. L. (2004) Aromatic interactions in peptides. *Biopolymers 76*, 435–445.
29. Favre, M., Moehle, K., Jiang, L., Pfeiffer, B., and Robinson, J. A. (1999) Structural mimicry of canonical conformations in antibody hypervariable loops using cyclic peptides containing a heterochiral diproline template. *J. Am. Chem. Soc. 121*, 2679–2685.
30. Dhanasekaran, M., Prakash, O., Gong, Y. X., and Baures, P. W. (2004) Expected and unexpected results from combined β-hairpin design elements. *Org. Biomol. Chem. 2*, 2071–2082.
31. Eidenschink, L., Kier, B. L., Huggins, K. N. L., and Andersen, N. H. (2009) Very short peptides with stable folds: Building on the interrelationship of Trp/Trp, Trp/cation, and Trp/backbone-amide interaction geometries. *Proteins: Struct., Funct., Bioinf. 75*, 308–322.
32. Guvench, O., and Brooks, C. L.III (2005) Tryptophan side chain electrostatic interactions determine edge-to-face vs parallel-displaced tryptophan side chain geometries in the designed β-hairpin "trpzip2". *J. Am. Chem. Soc. 127*, 4668–4674.
33. Mirassou, Y., Santiveri, C. M., Perez de Vega, J. M., Gonzalez-Muniz, R., and Jimenez, M. A. (2009) Disulfide bonds versus Trp$\cdots$Trp pairs in irregular beta-hairpins: NMR structure of vammin loop 3-derived peptides as a case study. *ChemBioChem 10*, 902–910.
34. Jager, M., Dendle, M., Fuller, A. A., and Kelly, J. W. (2007) A cross-strand Trp-Trp pair stabilizes the hPin1 WW domain at the expense of function. *Protein Sci. 16*, 2306–2313.
35. Sreerama, N., and Woody, R. W. (2003) Structural composition of {beta} I- and {beta}II- proteins. *Protein Sci. 12*, 384–388.
36. Sreerama, N., and Woody, R. W. (2000) Circular dichroism of peptides and proteins, in Circular Dichroism Principles and Applications (Nakanishi, K., Berova, N., and Woody, R. W., Eds.) pp 601−620, Wiley-VCH, New York.
37. Dukor, R. K., and Keiderling, T. A. (1991) Reassessment of the random coil conformation: vibrational CD study of proline oligopeptides and related polypeptides. *Biopolymers 31*, 1747–1761.
38. Shi, Z., Woody, R. W., and Kallenbach, N. R. (2002) Is polyproline II a major backbone conformation in unfolded proteins? *Adv. Protein Chem. 62*, 163–240.
39. Haris, P. I. (2000) Fourier transform infrared spectroscopic studies of peptides: potentials and pitfalls, in Infrared Analysis of Peptides and Proteins: Principles and Applications, ACS Symp. Ser. (Ram Singh, B., Ed.) pp 54−95, American Chemical Society, Washington, DC.
40. Kubelka, J., and Keiderling, T. A. (2001) Differentiation of β-sheet forming structures: ab initio based simulations of IR absorption and vibrational CD for model peptide and protein β-sheets. *J. Am. Chem. Soc. 123*, 12048–12058.
41. Keiderling, T. A., and Silva, R. A. G. D. (2002) in Synthesis of Peptides and Peptidomimetics (Goodman, M., and Herman, G., Eds.) pp 715−738, Verlag, New York.
42. Chirgadze, Y. N., Shetopalov, B. V., and Venyaminov, S. Y. (1973) Intensities and other spectral parameters of infrared amide bands of polypeptides in the beta and random forms. *Biopolymers 12*, 1337–1351.
43. Takekiyo, T., Wu, L., Yoshimura, Y., Shimizu, A., and Keiderling, T. A. (2009) Relationship between hydrophobic interactions and secondary structure stability for Trpzip β-hairpin peptides. *Biochemistry 48*, 1543–1552.
44. Cochran, A. G., Skelton, N. J., and Starovasnik, M. A. (2002) Correction. *Proc. Natl. Acad. Sci. U.S.A. 99*, 9081–9082.
45. Hwang, T., and Shaka, A. J. (1995) Water suppression that works: excitation sculpting using arbitrary waveforms and pulsed field gradients. *J. Magn. Reson. 112A*, 275–279.
46. Delaglio, F., Grzesiek, S., Vuister, G. W., Zhu, G., Pfeifer, J., and Bax, A. (1995) NMRRipe: a multidimensional spectral processing system based on UNIX pipes. *J. Biomol. NMR 6*, 277–293.
47. Johnson, B. A., and Blevins, R. A. (1994) NMR View: A computer program for the visualization and analysis of NMR data. *J. Biomol. NMR 4*, 604–613.
48. Guntert, P., Mumenthaler, C., and Wuthrich, K. (1997) Torsion angle dynamics for NMR structure calculation with the new program DYANA. *J. Mol. Biol. 273*, 283–298.
49. DeGuzman, R. N., Goto, N. K., Dyson, H. J., and Wright, P. E. (2006) Structural basis for cooperative transcription factor binding to the CBP coactivator. *J. Mol. Biol. 355*, 1005–1013.
50. Hornak, V., Abel, R., Okur, A., Strockbine, B., Roitberg, A., and Simmerling, C. (2006) Comparison of multiple Amber force fields and development of improved protein backbone parameters. *Proteins: Struct., Funct., Bioinf. 65*, 712–725.
51. Osapay, K., and Case, D. A. (1991) A new analysis of proton chemical shifts in proteins. *J. Am. Chem. Soc. 113*, 9436–9444.
52. Laskowski, R. A., Rullmann, J. A. C., MacArthur, M. W., Kaptein, R., and Thornton, J. M. (1999) AQUA and PROCHECK-NMR: programs for checking the quality of protein structures solved by NMR. *J. Biomol. NMR 8*, 477–486.
53. Wishart, D. S., Sykes, B. D., and Richards, F. M. (1992) The chemical shift index: a fast and simple method for the assignment of protein secondary structure through NMR spectroscopy. *Biochemistry 31*, 1647–1651.
54. Wishart, D. S., Sykes, B. D., and Richards, F. M. (1991) Relationship between nuclear magnetic resonance chemical shift and protein secondary structure. *J. Mol. Biol. 222*, 311–333.
55. Roy, A., Bour, P., and Keiderling, T. A. (2009) TDDFT modeling of the circular dichroism of coupled aromatic residues for a tryptohan zipper peptide. Chirality (in press).
56. Kiehna, S. E., Laughrey, Z. R., and Waters, M. L. (2007) Evaluation of a carbohydrate-π interaction in a peptide model system. *Chem. Commun.*, 4026–4028.
57. Tatko, C. D., and Waters, M. L. (2003) The geometry and efficacy of cation-π interactions in diagonal positions of a designed β-hairpin. *Protein Sci. 12*, 2443–2452.